ASSESSING THE SPATIAL VARIATION OF AEROSOL OPTICAL DEPTH AND ITS RELATIONSHIP WITH LAND USE/LAND COVER IN KATHMANDU VALLEY, NEPAL

Dibikshya Shrestha[1], Aayush Chand[1], Prejika Thapa[1], Bibek Ojha[1]

[1]Department of Geomatics Engineering, Pashchimanchal Campus, IOE, Tribhuvan University, Nepal

jbdibikshyashrestha@gmail.com, aayushchand123321@gmail.com,
thapapreji@gmail.com, bibekojha07@gmail.com

ABSTRACT

Aerosols play a crucial role in influencing atmospheric processes, air quality, and human health. Understanding the relationship between land use/land cover (LULC) and aerosol optical depth (AOD) is essential for developing effective land management and air pollution mitigation strategies. This study investigates the spatial variation of AOD and its association with LULC in Kathmandu Valley, Nepal, during the summer season of 2023. MODIS AOD products and Landsat 8-derived indices, including the Normalized Difference Vegetation Index (NDVI), Normalized Difference Built-up Index (NDBI), and Normalized Difference Water Index (NDWI), were utilized for this purpose. Spatial analysis revealed that lower AOD values were observed over forested areas, while higher concentrations were associated with water bodies, grasslands, and built-up areas. Correlation and regression analyses confirmed a negative relationship between vegetation cover and AOD, and a positive association between built-up areas, water surfaces, and aerosol loading. The study highlights the significant influence of LULC on aerosol distribution and provides essential information for land management and air pollution mitigation strategies.

KEYWORDS: Aerosol Optical Depth, NDVI, NDBI, NDWI, LULC, Kathmandu Valley, Remote Sensing, Air Quality

1. INTRODUCTION

Aerosols, fine solid or liquid particles present within the atmosphere, have a significant influence over environmental conditions, air quality, and public health. They play a vital role in radiative forcing, affecting both local and global climatic conditions by causing variations in the balance of solar radiation (Kaufman et al., 2005; Xie & Sun, 2021). Air pollution constitutes various components, primarily including airborne particulate matter (PM) and gaseous pollutants such as ozone (O3), nitrogen dioxide (NO2), volatile organic compounds (like benzene), carbon monoxide (CO), sulfur dioxide (SO2), among others (Newby et al., 2015), (Article, 2002). Fine particulate matter, specially PM2.5, with diameter less than 2.5 micrometers, has adverse effects on human health, affecting respiratory and cardiovascular diseases. As per the World Health Organization, over seven million people annually suffer diseases related to PM2.5 exposures (WHO, 2018). So, it is important to understand the aerosol behavior and its driving factors, centrally in urbanized and rapidly developing regions where there is an increment in aerosol concentrations due to both natural and anthropogenic sources. Globally, aerosol optical depth (AOD) has been on the rise in industrialized and densely populated regions. Satellite observations and ground-based measurements indicate the increasing trends over Asia, Africa and parts of Latin America, driven by urbanization, vehicular emission. Industrial activities and biomass burning (Van Donkelaar et al., 2013).

Kathmandu Valley, Nepal, is experiencing increasing urbanization, vehicular emissions, and agricultural activities that significantly influence air quality and aerosol distribution in the surrounding atmosphere. The valley's topography, evolving weather conditions, and rapid urban development, lead to intricate aerosol trends that vary both in space and time. Various research has resulted that Aerosol Optical Depth (AOD), which is a measure of the overall concentration of aerosols in the atmosphere, is strongly influenced by land use and land cover (LULC) configurations (Li et al., 2014; He et al., 2016). Land use

changes, especially urban expansion, deforestation, and agricultural intensification have resulted to directly affect aerosol concentrations and its distribution, resulting in increasing air pollution levels (Guo et al., 2012; Xie & Sun, 2021).

Satellite-derived products such as from the Moderate Resolution Imaging Spectroradiometer (MODIS) have proved to be essential in effective monitoring of aerosols at a regional scale. MODIS derived aerosol products have proven to provide consistent, sustainable, and large-scale observations of Aerosol Optical Depth (AOD), making them useful for analyzing aerosol shifts in both time and space (Gupta et al., 2006; Levy et al., 2013). These products offer spatial resolutions of up to 1 km, which allow for more detailed urban areas analysis given their global coverage and availability over two decades, MODIS AOD data have become a standard reference for numerous air quality and urban environmental studies (Remer et al., 2005).

The Kathmandu Valley's aerosol concentrations are influenced by various factors, including urbanization, industrial emissions, and transportation. Previous studies have highlighted the spatial variability of aerosol distribution in urban areas, where dense urban environments with high built-up areas generally tend to have high aerosol concentrations (Li et al., 2014). While areas with vegetation and natural terrains generally show lower aerosol levels due to natural filtration processes (Liu, X., et al. 2018). These variations are also influenced by topography, where lower-lying areas tend to accumulate aerosols due to limited ventilation and increased atmospheric stability (Xie & Sun, 2021).

Kathmandu Valley lacks in detailed studies on AOD variations, as well in relation with LULC, so our research aims to fill this gap by investigating the relationship between aerosol concentration and land cover patterns across the valley. This study will utilize remote sensing data, specifically Landsat 8 imageries and MODIS aerosol products, to analyze the spatial variation of AOD in Kathmandu Valley during the summer of 2024. The study objectives include:

1. Monitoring the spatial variation of AOD during the summer of 2024 and identifying key patterns in aerosol concentration.
2. Quantifying the correlations between AOD values and LULC-related variables, including vegetation indices such as NDVI (Normalized Difference Vegetation Index) and NDBI (Normalized Difference Built-up Index), and NDWI (Normalized Difference Water Index).
3. Assessing the influence of urbanization, agricultural land use, and natural environments on the spatial distribution of AOD.

By understanding the relationship between LULC and AOD in Kathmandu Valley, these findings will help improve land use management, inform air quality control strategies, and ultimately support efforts to reduce aerosol-related pollution in the valley.

2. MATERIALS AND METHODS

2.1 Study Area

This Study focuses on Kathmandu Valley (Figure 1), a bowl-shaped basin in the lesser Himalayas of central Nepal, spans 933.73 km² between 27.403° N and 27.818° N latitude and 85.189° E and 85.5657° E longitude. Its valley floor averages 1,425 m above mean sea level and is enclosed by the Shivapuri (2,732 m), Phulchowki (2,695 m), Nagarjun (2,095 m), and Chandragiri (2,551 m) ranges. The Bagmati River flows through the basin, which includes the administrative districts of Kathmandu, Bhaktapur, and Lalitpur.

A subtropical continental semi-humid climate (mean annual temperature ~18.3 °C; rainfall ~1,440 mm) and the bowl-shaped topography promote pollutant accumulation from biomass burning, vehicular emissions, and construction dust. Its diverse land cover and complex terrain provide an ideal setting to examine how vegetation, urban, agricultural, and water bodies influence Aerosol Optical Depth.

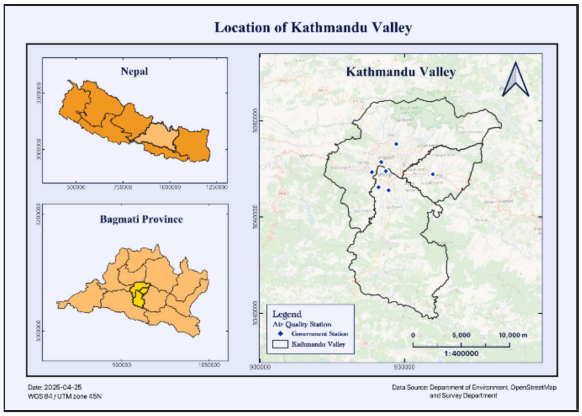

Figure 1. Location of Kathmandu Valley

2.2 Data Sources and Preprocessing

2.2.1 MODIS AOD: Processed in Google Earth Engine (GEE) by filtering the MCD19A2 granules for the Kathmandu Valley boundary and the period February 1 to July 1, 2023. We selected the Optical_Depth_055 band, applied a scale factor of 0.001, computed a seasonal mean composite, and clipped it to the study area.

2.2.2 Landsat 8 Surface Reflectance: Using GEE, Collection 2 Level-2 images with <10% cloud cover were filtered by date and region. Bands SR_B3 (Green), SR_B4 (Red), SR_B5 (NIR), and SR_B6 (SWIR1) were exported as seasonal mean rasters at 1 km resolution after compositing and reprojection to EPSG:32645.

2.2.3 Local Processing Environment: In Google Colab, we installed and imported Python packages—rasterio, numpy, pandas, geopandas, shapely, scikit-learn, matplotlib—for raster resampling, extraction, and statistical analysis after data export from GEE.

2.3 Derivation of Spectral Indices

Landsat 8 Collection 2 Level-2 images were processed in Google Earth Engine (GEE) to derive spectral indices representing vegetation, built-up structures, and surface water. These images provide surface reflectance values, which were converted using a radiometric scaling formula: applying a multiplier of 0.0000275 and an offset of –0.2 to convert raw DN values to reflectance.

Three indices were computed for each image:

- **NDVI (Normalized Difference Vegetation Index):**

  NDVI (Normalized Difference Vegetation Index) is used to assess vegetation cover based on the difference between near- infrared (NIR) and red reflectance.

  $$NDVI = (NIR - Red) / (NIR + Red) \quad (1)$$

- **NDBI (Normalized Difference Built-up Index):** NDBI (Normalized Difference Built-up Index) is used to assess built-up areas based on shortwave infrared (SWIR1) and NIR reflectance.

  $$NDBI = (SWIR1 - NIR) / (SWIR1 + NIR) \quad (2)$$

- **NDWI (Normalized Difference Water Index):**

  NDWI (Normalized Difference Water Index) is used to detect water bodies based on green and NIR reflectance.

  $$NDWI = (Green - NIR) / (Green + NIR) \quad (3)$$

In Landsat 8 Collection 2 Level-2 images, Red = SR_B4, Green = SR_B3, NIR = SR_B5, and SWIR1 = SR_B6. These indices were calculated per scene after cloud filtering and composited to create seasonal mean images that were then reprojected to 1 km resolution (EPSG:32645) and exported as GeoTIFFs for further analysis.

2.4 Data Integration and Preprocessing

All data layers were projected to EPSG:32645 and resampled to match the 30 m resolution of the LULC raster. MODIS AOD and Landsat indices were resampled using bilinear interpolation in Python. This alignment ensured pixel-level consistency for statistical correlation analysis.

2.5 Statistical Analysis

Pixel-level values of AOD, NDVI, NDBI, NDWI, and LULC were extracted and analyzed in Python. Summary statistics (mean, min, max, std. dev.) of AOD were calculated for each LULC class. Area proportions were derived using pixel counts and the known pixel area (0.0009 km^2 for 30m resolution). Correlation coefficients were computed between AOD and LULC-related indicators. Regression analysis was conducted to visualize and quantify the relationships between AOD and the selected indices.

3. RESULTS

3.1 Land Use/Land Cover Composition

Land use/ Land Cover were classified using the Maximum Likelihood method in ArcMap. Five classes were defined: water body, built-up areas, forest, farmland and grassland. Training samples were digitized manually. Accuracy was accessed using over 50 validation points per class via Google Earth imagery. The classification of land use/land cover revealed that grassland (27.90%), forest (25.58%), and farmland (25.00%) dominate the Kathmandu Valley, while built-up areas and water bodies occupy 20.86% and 0.66% of the total area respectively (Table 2). The spatial distribution (Figure 3) of these categories illustrates that grassland and forest areas are mainly located on the periphery, while built-up areas are concentrated in the valley core.

Table 2. Area statistics of LULC types

LULC Type	Area (km^2)	Proportion (%)
Water body	6.17	0.66
Built-up areas	194.62	20.86
Forest	238.72	25.58
Farmland	233.29	25.00
Grassland	260.37	27.90

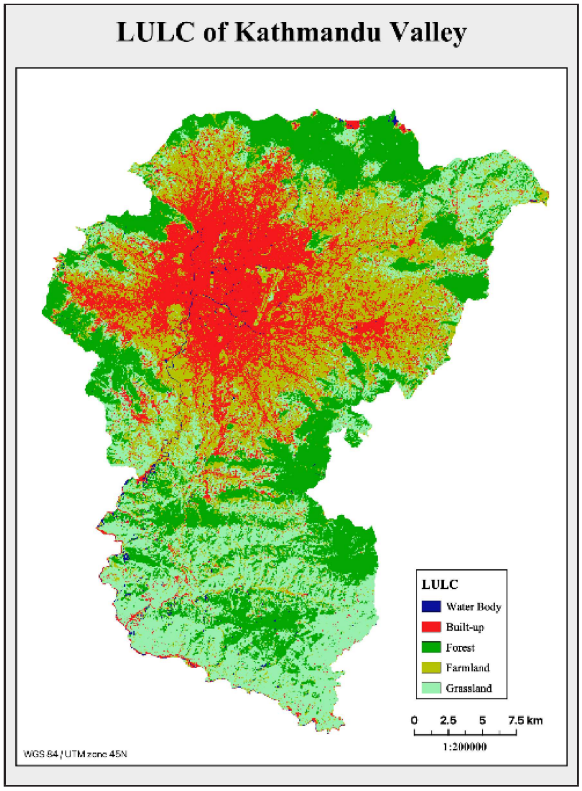

Figure 3. LULC of Kathmandu Valley

3.2 AOD Distribution by LULC Class

Analysis of mean AOD values (Table 4) highlights pronounced differences among LULC types. Water bodies record a mean AOD of 0.451 (SD = 0.051), as these low-lying surfaces trap aerosols under stable atmospheric conditions. Grasslands follow with a mean of 0.447 (SD = 0.062), reflecting dust entrainment in exposed terrains during the dry season. Built-up areas have a mean AOD of 0.441 (SD = 0.025), consistent with urban emissions from vehicles and construction activities. Farmland shows a mean of 0.433 (SD = 0.031), influenced by tillage, harvesting, and biomass burning. Forests exhibit the lowest mean AOD at 0.401 (SD = 0.048), underscoring canopy uptake and deposition processes.

Table 4. AOD statistics in different LULC type

LULC Type	Min	Max	Mean AOD	SD
Built-up areas	0.320	0.622	0.441	0.025
Farmland	0.305	0.621	0.433	0.031
Forest	0.304	0.618	0.401	0.048
Grassland	0.304	0.622	0.447	0.062
Water body	0.324	0.621	0.451	0.051

The spatial pattern (Fig. 5) demonstrates that transitional zones—particularly grassland adjacent to urban fringes and water margins—experience elevated and highly variable aerosol loading, combining natural dust sources and anthropogenic contributions. In contrast, built-up areas maintain relatively uniform AOD levels, indicative of steady emission rates. Forested corridors consistently show lower aerosol burdens, supporting their critical role as natural sinks in the valley's aerosol dynamics.

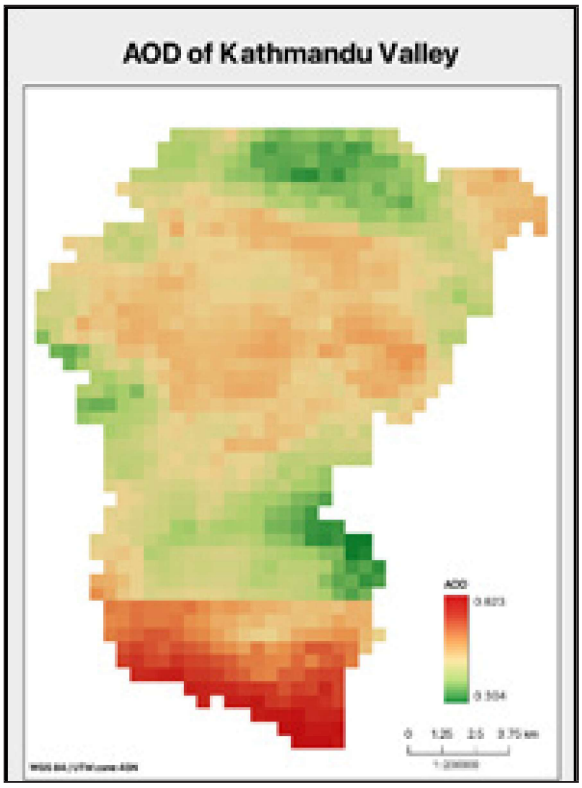

Figure 4. Spatial distribution maps of AOD

3.3 AOD and Vegetation/Built-up/Water Indices

The interaction between AOD and surface characteristics is further elucidated by comparing aerosol levels with three spectral indices (Figs. 7–9; Table 6). NDVI values above 0.5 in peripheral forests coincide with the lowest AOD readings (<0.42), illustrating the effectiveness of dense vegetation in sequestering particles. Conversely, NDBI peaks (up to 0.45) in central Kathmandu correspond to zones of elevated AOD (>0.44), highlighting urban emissions as a primary aerosol source. NDWI, though generally low (<0.2), shows localized increases near water bodies where AOD also rises, suggesting that moisture-rich areas may experience aerosol retention under stable atmospheric layers.

Quantitatively, Pearson correlations (Table 6) reveal a significant inverse relationship between AOD and NDVI (r = –0.168), affirming the noise-reduction capacity of green cover. A strong positive correlation between AOD and NDBI (r = 0.360) highlights built environments as hotspots for particulate matter. The positive although weaker correlation with NDWI (r = 0.169) points to the role of surface moisture and topographic depressions in modulating aerosol concentrations.

When examining binary LULC metrics, the proportion of forest cover (PerForest) shows the highest negative correlation with AOD (r = –0.361), while the proportion of built-up land (PerCon.) exhibits a positive correlation (r = 0.115). These results collectively demonstrate that spectral indices can serve as effective proxies for predicting spatial patterns of aerosol loading across heterogeneous landscapes.

Table 6. Correlation coefficients between AOD and LULC-related variables

Variable	AOD
NDVI	-0.168
NDBI	0.360
NDWI	0.169
PerWater	0.034
PerCon.	0.115
PerForest	-0.361
PerFarm	0.030
PerGreen	0.211

3.4 Regression Analysis

The linear regression plots illustrate the degree of relationship between AOD and NDVI, NDBI, and NDWI. AOD shows a slight negative trend with NDVI, and modest positive trends with both NDBI and NDWI. These trends visually support the statistical outcomes of the Pearson correlation analysis, providing intuitive evidence that dense vegetation helps lower AOD, while built-up and lowland water-prone regions may accumulate aerosols.

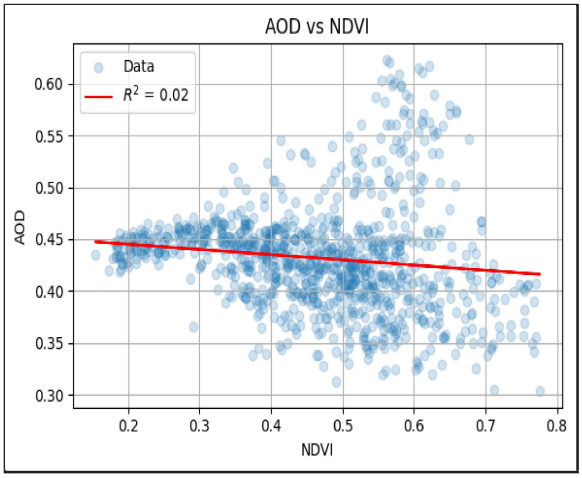

Figure 10. Regression plot of AOD vs NDVI

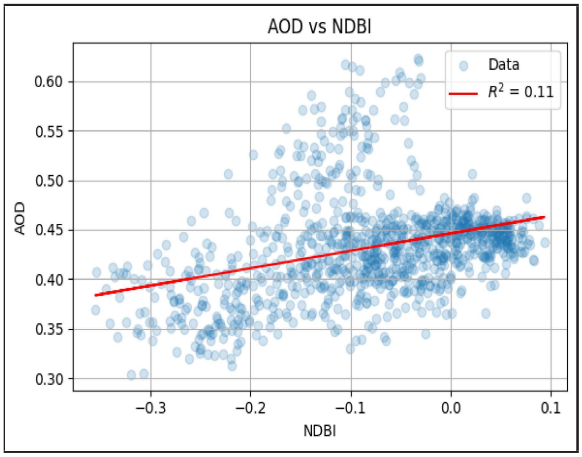

Figure 11. Regression plot of AOD vs NDBI

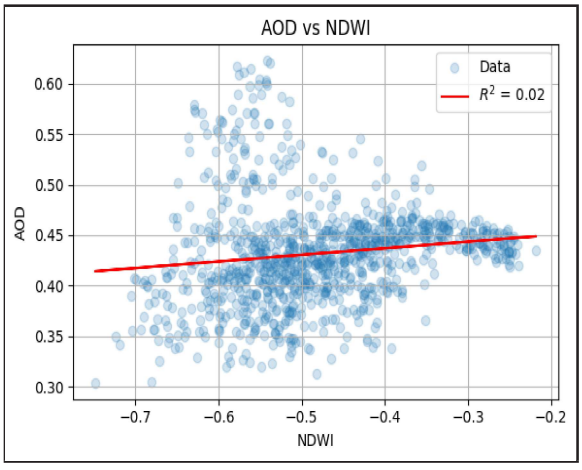

Figure 12 Regression plot of AOD vs NDWI

4. DISCUSSION

The spatial variation of Aerosol Optical Depth (AOD) in Kathmandu Valley from February to July 2023 reflects the influence of land use and land cover (LULC) on aerosol concentrations. Mean AOD values ranged from 0.401 in forested areas to 0.451 over water bodies, indicating moderate aerosol loading. A low overall standard deviation (0.0536) suggests relatively consistent spatial distribution despite varying terrain and land cover.

Vegetated areas such as forests recorded the lowest AOD levels, supported by negative correlations with NDVI (−0.127) and PerForest (−0.217), indicating that dense vegetation helps reduce aerosol concentrations through natural filtration and dry deposition (Liu et al., 2018). In contrast, built-up areas exhibited higher AOD values, with Built-up areas and NDBI showing positive correlations (0.115 and 0.337, respectively), highlighting the impact of urbanization and human activities like traffic and construction on air pollution.

Interestingly, water bodies showed relatively high mean AOD and the largest variability (standard deviation 0.078), likely due to their low-lying locations that favor aerosol entrapment. The weak positive correlation with NDWI (0.133) may also reflect influences of topography and atmospheric stability.

Agricultural lands showed a notable aerosol presence, with a mean AOD of 0.433 and the highest correlation (0.218) among all LULC types. This is likely linked to seasonal agricultural practices such as tilling, harvesting, and biomass burning during the pre-monsoon period.

While these findings underscore the role of LULC in aerosol distribution—with vegetation acting as a mitigating factor and urban/agricultural areas contributing to higher concentrations—there are notable limitations. The use of seasonal averages may mask short-term variations in AOD, and the MODIS AOD product's coarse resolution could reduce accuracy when matched with finer-scale Landsat-based indices. Furthermore, the absence of meteorological data such as wind speed, temperature, or humidity limits understanding of aerosol dispersion dynamics.

Future research should incorporate higher temporal resolution data, integrate meteorological parameters, and validate findings with ground-based air quality monitoring to enhance reliability and policy relevance.

5. CONCLUSION

By integrating MODIS AOD products with Landsat-derived NDVI, NDBI, and NDWI indices, this study has clearly demonstrated that land cover types exert significant control over aerosol loading in Kathmandu Valley. Forested areas recorded the lowest mean AOD (0.401), underscoring the efficacy of dense vegetation in removing particles, while grasslands and water bodies exhibited the highest levels (0.447 and 0.451, respectively) due to surface dust entrainment and topographic trapping. Built-up zones showed consistently elevated AOD (0.441), highlighting urban emissions as key contributors to poor air quality. Correlation and regression analyses of AOD ($r = -0.168$ for NDVI; $r = 0.360$ for NDBI; $r = 0.169$ for NDWI) reinforce these spatial patterns.

Although the use of seasonal composites and resampled rasters may obscure short-term dynamics, and the exclusion of meteorological variables limits dispersion insights, the robust relationships observed advocate for nature-based solutions and targeted land use policies. Specifically, expanding urban green corridors, controlling construction dust, and protecting remaining forest patches can help mitigate aerosol pollution. Future work should integrate in-situ air quality measurements, high-frequency satellite observations, and local meteorological data to refine temporal analyses and extend the methodology beyond Kathmandu Valley for national-scale air quality management.

REFERENCES

Guo, J., Zhang, X., Che, H., Gong, S., An, X., Cao, C., ... & Zhang, W. (2012). Spatial and temporal variations of aerosol optical depth and their correlation with influencing factors over central China. *Atmospheric Research*, *104–105*, 96–106. https://doi.org/10.1016/j.atmosres.2012.01.011

He, Y., Xu, H., Sun, Z., Zhang, Y., Wang, Y., & Gu, J. (2016). Spatiotemporal variations of aerosol optical depth in relation to land use and socio-economic factors. *Science of The Total Environment*,*568*,689–699. https://doi.org/10.1016/j.scitotenv.2016.06.152

Kaufman, Y. J., Tanré, D., Remer, L. A., Vermote, E. F., Chu, A., & Holben, B. N. (2005). The effect of aerosol particles on the radiation budget of the Earth and the implications for climate change. *Atmospheric Environment*, *39*(1), 1–8. https://doi.org/10.1016/j.atmosenv.2004.09.027

Li, Y., Wang, Y., Wang, J., & Wang, X. (2014). Aerosol optical depth and its relation to land use/land cover in urban areas. *Atmospheric Environment*, *94*, 547–555. https://doi.org/10.1016/j.atmosenv.2014.06.009

Newby, D. E., Mannucci, P. M., Tell, G. S., Baccarelli, A. A., Brook, R. D., Donaldson, K., ... & Mills, N. L. (2015). Expert position paper on air pollution and cardiovascular disease. *European Heart Journal*, *36*(2), 83–93. https://doi.org/10.1093/eurheartj/ehu458

van Donkelaar, A., Martin, R. V., Spurr, R. J. D., Drury, E., Remer, L. A., Levy, R. C., & Wang, J. (2013). Optimal estimation for global ground-level fine particulate matter concentrations. *Journal of Geophysical Research: Atmospheres*, *118*(11), 5621–5636. https://doi.org/10.1002/jgrd.50479

World Health Organization. (2018). *Ambient (outdoor) air quality and health*. https://www.who.int/news-room/fact-sheets/detail/ambient-(outdoor)-air-quality-and-health

Xie, Q., & Sun, Q. (2021). Monitoring the spatial variation of aerosol optical depth and its correlation with land use/land cover in Wuhan, China: A perspective of urban planning. *International Journal of Environmental Research and Public Health*, *18*(3), 1132. https://doi.org/10.3390/ijerph18031132

Article, O. (2002). Personal exposure monitoring of particulate matter, nitrogen dioxide, and carbon monoxide, including susceptible groups. *[Journal Name]*, *[Volume(Issue)]*, 671–679.

AUTHOR INFORMATION

Name : **Dibikshya Shrestha**

Academic Qualification : BE in Geomatics Engineering

Organization : IT Maps

Current Designation : Intern